Chapter

Performance and Applications of Lithium Ion Capacitors

Xiaogang Sun, Wei Chen, Xu Li, Jie Wang, Hao Hu, Guodong Liang, Yapan Huang and Chengcheng Wei

Abstract

Lithium-ion capacitors (LICs) have a wide range of applications in the fields of hybrid electric vehicles (HEVs) and electric vehicles (EVs) for their both high energy density and high power density. Lithium-ion capacitors have become a potential alternative for next-generation chemical energy storage equipment owing to high energy density, high power density, and excellent cycle performance. The prelithiated multiwalled carbon nanotubes (MWCNTs) electrode was prepared by internal short circuit (ISC) and doping to intercalate lithium into MWCNTs. SLMP and lithium metal were used as lithium resources, respectively. The prelithiated carbon nanotubes were used as anode and activated carbon electrode as cathode. The capacitors were assembled in a glove box filled with argon. The prelithiated MWCNTs electrode eliminated irreversible capacity and improved substantially electrochemical performance of lithium-ion capacitors.

Keywords: prelithiation, stabilized lithium metal powder, graphite, multiwalled carbon nanotubes, activated carbon, lithium-ion capacitors

1. Introduction

The fossil energy's shortage and the use of fossil fuels cause environmental pollution and climate anomalies. The development and utilization of new energy sources, especially renewable energy, such as solar energy, wind energy, biomass, and hydrogen energy, have attracted increasing attention [1, 2]. And the development of new energy and energy storage equipment has become the focus of the investigation [3, 4]. Lithium-ion batteries (LIBs) and electrochemical capacitors (EC) are two important chemical energy storage devices. LIBs have high energy density but lower power density and cycle performance. EC has high power density and long cycle performance, but much lower energy density than the LIBs [5–8].

Lithium-ion capacitors, which combined the merits of lithium-ion batteries and electrochemical capacitors, are a new type of energy storage devices between the lithium-ion batteries and the electrochemical capacitors [9, 10]. In LICs, the anions adsorption and desorption in the electrolyte occurs on surface of positive electrode and simultaneously cations redox reaction occurred in the negative electrodes [11–15]. The ionic adsorption of electrical double layer and the faradaic electrochemical process (redox reaction) caused by lithium-ion intercalation and deintercalation contribute to high energy and powder density of lithium-ion capacitors than traditional capacitors [16–20].

In the carbon-based lithium-ion capacitors, the lithium ions are mainly derived from the electrolyte. But the solid-electrolyte interface (SEI) film formed during cycles will consume an amount of lithium ions which are irreversibly embedded in negative materials. That will bring down the capacity and cycle performance of LICs. So it is particularly important for the lithium predoping in negative electrode [21]. MWCNTs composed of unique one-dimensional systems with nanostructure have better stability, excellent conductivity, and lithium capacitance. It has become a popular research object for lithium-ion batteries [22]. SLMP applied to negative electrode can effectively prevent the problem of lithium ions deficiency and increase the capacity and rate performance of the LICs [23]. There is a potential difference between carbon electrode and lithium metal, which will promote the continuous flow of lithium ions into the carbon electrode when the carbon electrode and lithium metal are connected by short circuiting [9, 24, 25]. The final potential of the carbon anode will drop close to 0 V (vs. Li/Li+). Here, we introduce two new type LICs with different preintercalated lithium anodes.

It is generally known that graphite has a high theoretical Li intercalation capacity and widely was used as anode materials for lithium-ion capacitors because of natural abundance and relatively low cost [26–30]. However, lithium-ion intercalation tended to the same direction, and the dynamics of lithium-ion intercalation is slow. So it is difficult to perform charge/discharge work for lithium-ion capacitor at high current density with a poor rate performance [31, 32]. Compared to graphite, MWCNTs have higher stability. In this chapter, we report internal short circuit (ISC) approach was applied to high-performance LICs with activated carbon as cathode and prelithiated multiwalled carbon nanotubes/graphite composite as anode. Electrochemical performance of lithium-ion capacitors was investigated.

2. Fabrication and characterization of MWCNTs

MWCNTs were prepared by chemical vapor deposition (CVD), and benzene (Aladdin Co. Ltd., Shanghai) was used as carbon source, ferrocene (Aladdin Co. Ltd., Shanghai) as catalyst, and thiophene (Aladdin Co. Ltd., Shanghai) as accelerant. Ferrocene and thiophene were added into benzene and stirred uniformly; the flow rate was controlled by a micropump. Hydrogen and argon were used as carrier gas. The flow rate was controlled by a mass flow meter. The carbon source was fed into reactor with carrier gas. The MWCNTs were synthesized in a tube furnace with appropriate contents of ferrocene and thiophene and the ratio of benzene to

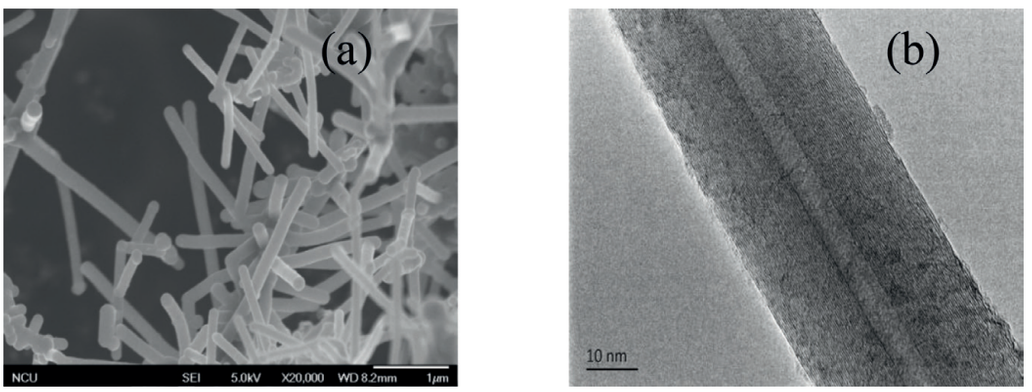

Figure 1.
(a) FESEM and (b) HRTEM images of MWCNTs.

hydrogen in a certain temperature gradient. The obtained MWCNTs were further graphitized under the condition of vacuum at 2800°C for 24 h with the heating rate of 10°C/min. Finally, the graphitized MWCNTs were milled in a planetary ball mill at 200 r/min for 3 h [33].

Figure 1(a) showed FESEM image of MWCNTs. The MWCNTs presented linear and smooth structure. The diameters of the MWCNTs range from 100 to 120 nm with a large aspect ratio, and the MWCNTs have a small probability of bending around each other in space. Because of this particular microstructure makes the MWCNTs dispersed easily, simultaneously excellent conductivity and lithium-ions adsorption capacity, and other characteristics. **Figure 1(b)** showed HRTEM image of graphitized MWCNTs; the MWCNTs exhibited one-dimensional hollow structure, smooth wall, low defects, thin wall thickness, and regular and orderly arrangement of carbon atoms

3. SLMP/MWCNTs composite anode for lithium-ion capacitors

3.1 Experiment

3.1.1 Preparation of cathode electrode

The activated carbon (AC) was dispersed by sonication in N-methyl-2-pyrrolidone (NMP) for 2 h. The surfactant of polyvinylpyrrolidone (PVP, YueMei chemical Co. Ltd., Guangzhou) was added to improve the dispersion performance. The polyvinylidene fluoride (PVDF) was used as binder. The super carbon black (SP) was added to improve the conductivity. The activated carbon slurry was completed after a high-speed (FA25) cutting under 10,000 r/min for 1 h, and the mass ratio of AC:SP:PVDF was 85:5:10. The prepared slurry was coated on Al foil and dried at 60°C under vacuum, and cut into a disc of 14 mm diameter.

3.1.2 Preparation of anode electrode

The MWCNT powders were dispersed by sonication in N-methyl-2-pyrrolidone (NMP) for 2 h. The surfactant of polyvinylpyrrolidone was added to improve the dispersion performance. The polyvinylidene fluoride (PVDF) was used as binder. The slurry was completed after a high-speed (FA25) cutting under 10,000 r/min for 1 h. The mass ratio of MWCNTs:SP:PVDF was 8:1:1. The prepared slurry was coated on Cu foil and dried at 60°C under vacuum. A mixture of 0.5% polystyrene (PS) and 0.5% styrene butadiene rubber (SBR) was selected as a polymer binder, xylene as a solvent, and two groups were mixed to produce a binder solution. SLMP (FMC Corporation) was dispersed in the binder solution to obtain SLMP suspension with 0.5 wt%. Then the SLMP suspension was evenly coated on anode. After dried in vacuum, the SLMP coating is pressed between two glass plates for activating SLMP and then cut into a disc of 14 mm diameter.

3.1.3 Fabrication and characterization of lithium-ion capacitors

The two-electrode CR-2025 button lithium-ion capacitors were assembled with activated carbon as cathode and SLMP/MWCNT composites as anode in an argon-filled dry glove box. The electrolyte was 1 mol/L $LiPF_6$ in a mixed solvent system of EC/DMC (ethylene carbonate/diethyl carbonate) at a ratio of 1:1, and polypropylene microporous membrane was used as the separator.

The MWCNTs were characterized by field-emission scanning electron microscopy (FE-SEM, JSM-6701F), transmission electron microscopy (TEM, JEOL JEM-2010FEF), X-ray diffraction (XRD, DI SYSTEM), Raman spectrometer (SENTERRA), and thermogravimetry (TGA, PYRIS DIAMOND). The galvanostatic charge-discharge test of lithium-ion capacitors was performed after placed at room temperature for 24 h by a cell tester (CT-3008W-5V5mA-S4).

3.2 Results and discussion

3.2.1 The micromorphology of SLMP and AC

Figure 2(a) showed the micromorphology of SLMP. The diameters of the SLMP range from 30 μm, and outside coated with a thin layer of Li_2CO_3 protective coating, which can exist in a relatively low air humidity environment. **Figure 2(b)** showed the micromorphology of AC; it was observed that AC particles show irregular morphology and the average size of the particles is about 4 μm.

3.2.2 XRD and Raman spectroscopy analysis of MWCNTs

Figure 3(a) showed the X-ray diffraction (XRD) pattern of MWCNTs. The main diffraction peaks of MWCNTs were both at 2θ = 26°, which coincide with the (002) planes. The main diffraction peak of MWCNTs is sharp and narrow, which indicates that the MWCNTs have a more regular and orderly arrangement of carbon atoms. Moreover, MWCNTs have a higher degree of crystallinity and conductivity. The

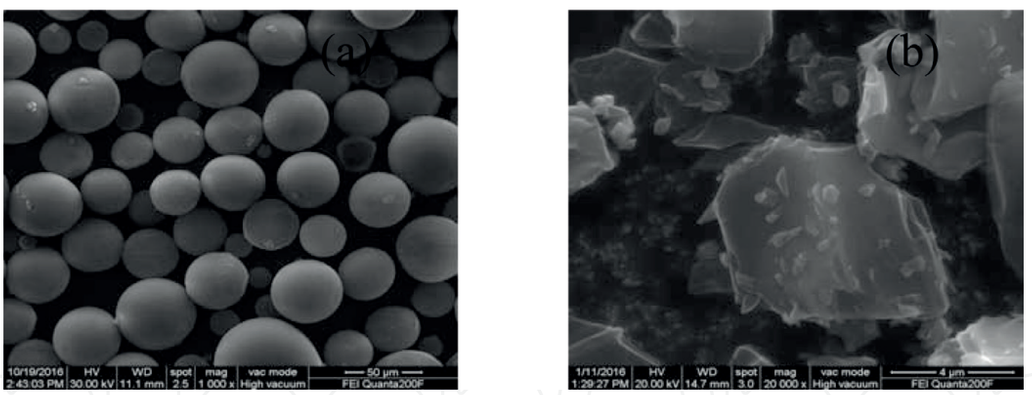

Figure 2.
Micromorphology of (a) SLMP and (b) AC.

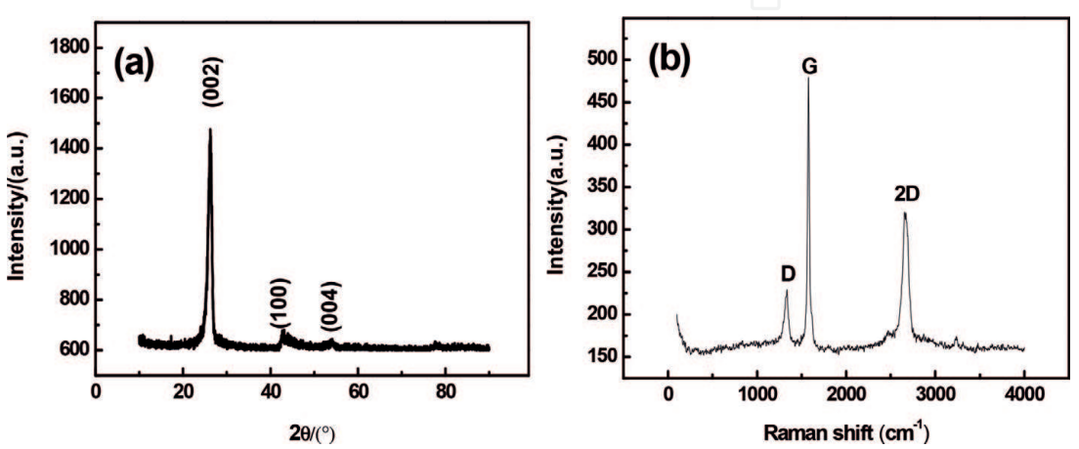

Figure 3.
XRD (a) and Raman spectroscopy (b) of MWCNTs.

(100) and (004) diffraction peaks are the catalyst components in the preparation of MWCNTs. **Figure 3(b)** showed the Raman spectroscopy of MWCNTs. There exhibited two distinct peaks corresponding to about 1351 cm-1D band and about 1585 cm-1G band, respectively. The MWCNTs have higher and sharper G peaks, which indicate that the degree of crystallinity and structure integrity of MWCNTs are great. In addition, the 2D peak appears at 2752 cm^{-1}, which indicates that the MWCNTs have higher degree of crystallinity.

3.2.3 TG of the MWCNTs

Figure 4 showed the TG curves of MWCNTs. The TG test was performed under air atmosphere with the heating rate of 5°C/min to 1000°C. The TG curves of MWCNTs were divided into two stages. In the first stage, the weight loss of 0.11% is caused by the oxidation of a small amount of amorphous carbon during the synthesis of MWCNTs. The weight loss of the second stage is caused by the ablation of impurities in the MWCNTs. The initial reaction temperature of MWCNTs was 585°C, which indicates that the antioxidant capacity and thermal stability of MWCNTs were great. Meanwhile, the residual amounts of MWCNTs were 0.2%, which confirm that the purity of these MWCNTs is great.

3.2.4 Galvanostatic charge and discharge

Figure 5(a) and **(b)** showed the galvanostatic charge-discharge curves of none-lithiated and prelithiated LICs at different current densities, respectively. The tests were performed using two-electrode system at voltage profile of 2–4 V. The energy density of LICs can be calculated by $E_{sp} = (C_{sp}{}^{*}V^{2})/2$ (C_{sp} represents the specific capacitance and V represents the discharge potential excluding IR drop). The power density of LICs can be calculated by $P_{sp} = E_{sp}/t$ (t represents the discharge time), and the specific capacitance C_{sp} can be calculated by the formula $C = (2I^{*}t)/(m^{*}\Delta V)$ (I represents the discharge current, m is the active material mass of a single pole, ΔV is the potential of discharge, and t is the discharge time). The charge-discharge curves of prelithiated LICs showed a good linear relationship and exhibited a shape of isosceles triangle. On the contrary, the charge-discharge curves of nonlithiated LICs presented a distorted shape, and the internal resistance obviously increases with the improving current density and the discharge time is obviously shortened, which related a poor

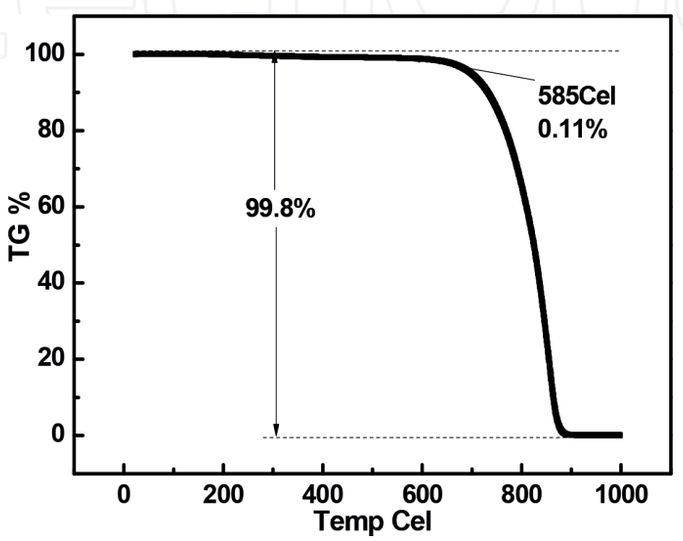

Figure 4.
TG curve of MWCNTs.

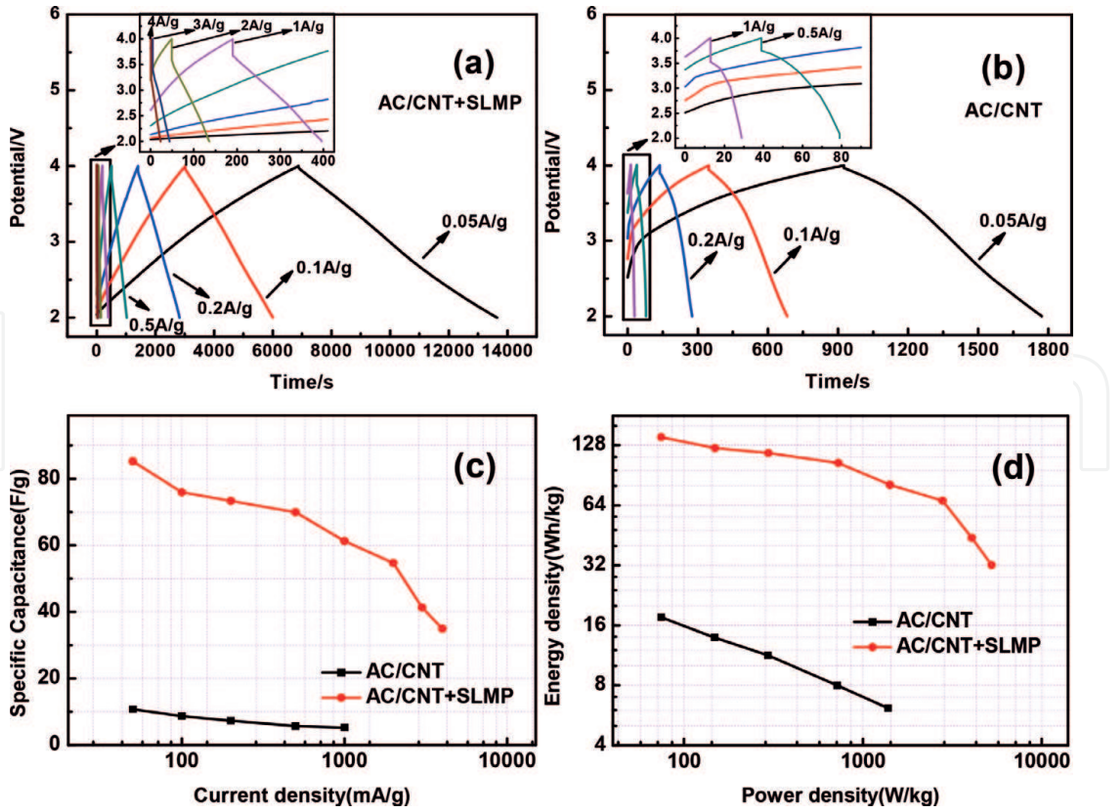

Figure 5.
Galvanostatic charge/discharge curves of LICs with nonlithiated (a) and prelithiated (b) specific capacitance with different current density (c) and the ragone plots (d) for the LICs.

power density. Generally, the power density of lithium-ion capacitors is determined by the negative materials; when the negative electrode consists of nonlithiated MWCNTs, the rate of intercalation and deintercalation of lithium ions is slow, resulting in a poor power density. The intercalation and deintercalation rate of lithium ions will be accelerated with the addition of SLMP. **Figure 5(c)** showed the discharging specific capacity at different rates. The prelithiated LICs showed higher discharging specific capacity and rate performance than those of nonlithiated LICs. The nonlithiated and prelithiated LICs exhibited discharging specific capacity of 10.74 and 85.18 F/g at current density of 0.1 A/g. **Figure 5(d)** showed the ragone plots of LICs. Prelithiated LICs presented the best electrochemical performance. The maximal energy density and power density of prelithiated LICs reached 140.4 Wh/kg and 5.25 W/kg in the range of current density from 0.05 to 4 A/g [34, 35].

Figure 6(a) showed the charge and discharge cycle performance of LICs with nonlithiated and prelithiated. The 3000 cycles test was performed in the range of 2~4 V at the current density of 0.4 A/g. After 3000 cycles of constant current charge and discharge, the cycling performance of LICs with nonlithiated drops significantly. In contrast, **Figure 6(b)** showed the discharge cycle performance of LICs with prelithiated after 3000 cycles. The capacitance retention still holds 82%, the charge and discharge curves without twist and distortion, which still maintained a good isosceles triangle shape and shows good cycle performance.

3.3 Conclusions

In the chapter, lithium-ion capacitors have been assembled with SLMP/MWCNTs composite as anode and activated carbon as cathode, respectively. The results showed that prelithiated LICs exhibit excellent electrochemical performance. The addition of SLMP to anode can increase the electrochemical

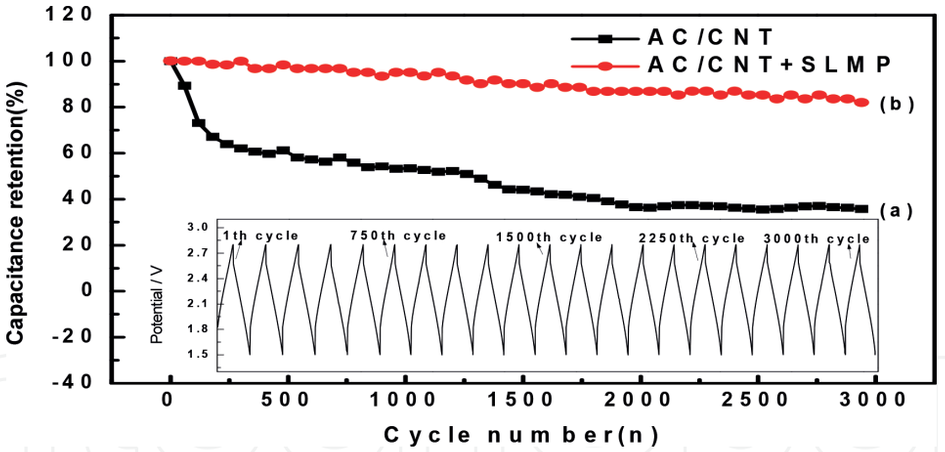

Figure 6.
Charge and discharge cycle performance of LICs with nonlithiated (a) and prelithiated (b).

performance of the LICs and eliminate irreversible capacity. Especially, the prelithiated LICs exhibited optimal electrochemical performance, with a specific capacity of 85.18 F/g at current density of 0.1 A/g, and the maximal energy and power density reached 140.4 Wh/kg and 5.25 W/kg in the range of current density from 0.05 to 4 A/g, respectively. After 3000 charge-discharge cycles, the prelithiated LICs maintained about 82% capacity retention rate, Therefore, the prelithiated LICs with a SLMP addition in the anode have a potential application for energy storage device.

4. Lithium-ion capacitors using prelithiated MWCNTs/graphite composite as anode

4.1 Experiment

4.1.1 The preparation of anode and prelithiation procedure

The slurry of composite active material (MWCNTs/graphite) was prepared by ultrasonically dispersing and high-speed shearing with super carbon black (SP) as conductive agent, polyvinylidene difluoride (PVDF) as binder, and NMP as solvent, with the ratio of 8:1:1. The slurry was coated on the copper foil. Then, the anode was dried at 60°C under vacuum for 12 h. The MWCNTs content in composite active material was 0, 25, 50, 75, 100 wt%, respectively. The prelithiation was accomplished through direct physical contact between as-prepared MWCNTs/graphite electrode and lithium metal with electrolyte in pressure; the degree of prelithiation was controlled by contact time.

4.1.2 The preparation of cathode

The ratio of AC:SP:PVDF is 8:1:1, subsequently followed by ultrasonically dispersing, high-speed shearing, and coating on aluminum foil. Then, the cathode was dried at 60°C under vacuum for 12 h and was cut into a disc of 14 mm diameter.

4.1.3 The fabrication of MWCNTs/Li half-cells and lithium-ion capacitors

The tailored MWCNTs/graphite anodes were used as working electrodes. Lithium foil was used as the counterelectrode and Celgard 2300 was used as the separator. The solution of 1.0 M LiPF6 in EC:DMC (1:1, vol.) was utilized as the electrolyte. Based

on the content of MWCNTs, the half-cells were signed as CNT0, CNT25, CNT50, CNT75, and CNT100, respectively. The two-electrode LICs were assembled with AC cathode and MWCNTs anode, and the corresponding LICs were recorded as LIC0, LIC25, LIC50, LIC75, LIC100. All cells were assembled in an argon-filled glove box.

4.1.4 Characterizations

The SEM of anode and that of cathode were characterized by FE-SEM (JSM-6701F). The electrochemical characterization of the LICs was performed by a cell tester (CT-3008W-5V5mA-S4). The specific capacitance was calculated based on total mass of the MWCNTs, graphite, AC, and SP.

4.2 Results and discussion

4.2.1 The SEM of anode and cathodes

Figure 7(a) shows the SEM image of AC anode, which shows irregular structure and occupies the vast majority of space. Meanwhile, SP uniformly dispersed between gaps of AC particles can provide good conductivity. **Figure 7(b)** shows the SEM image of graphite cathode, and **Figure 7(c)** shows the SEM image of MWCNTs/graphite composite cathode; comparison shows that MWCNTs and graphite are well connected and present a web-like network structure and three-dimensional conduction system. This structure was applied to the negative electrode to shorten the diffusion path of lithium ions and improve the kinetics of lithium-ion intercalation.

4.2.2 Galvanostatic charge and discharge

Figure 8(a) shows the first charge and discharge curves of raw MWCNTs and graphite half-cells at 1C rate; for graphite half-cells, the voltage plateau of SEI film formation is at about 0.7 V [36]. In comparison, for MWCNT half-cells, the

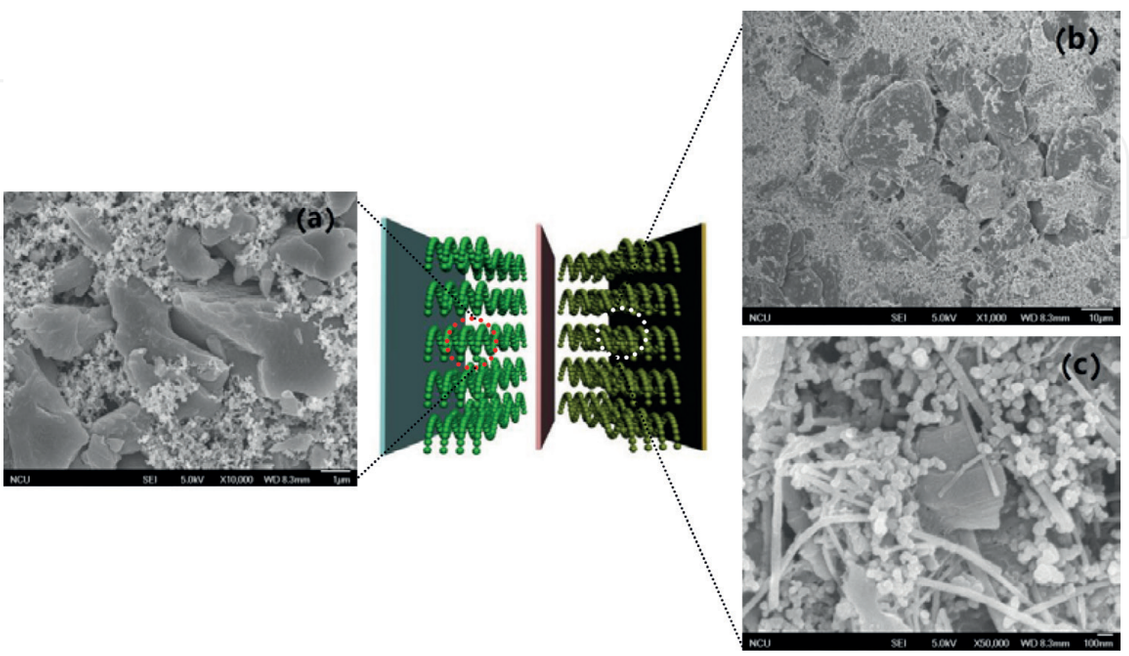

Figure 7.
Illustration of lithium-ion capacitors and corresponding SEM images of the electrode materials. (a) SEM image of AC anode, (b) SEM image of graphite cathode, (c) SEM image of MWCNTs/graphite composite cathode.

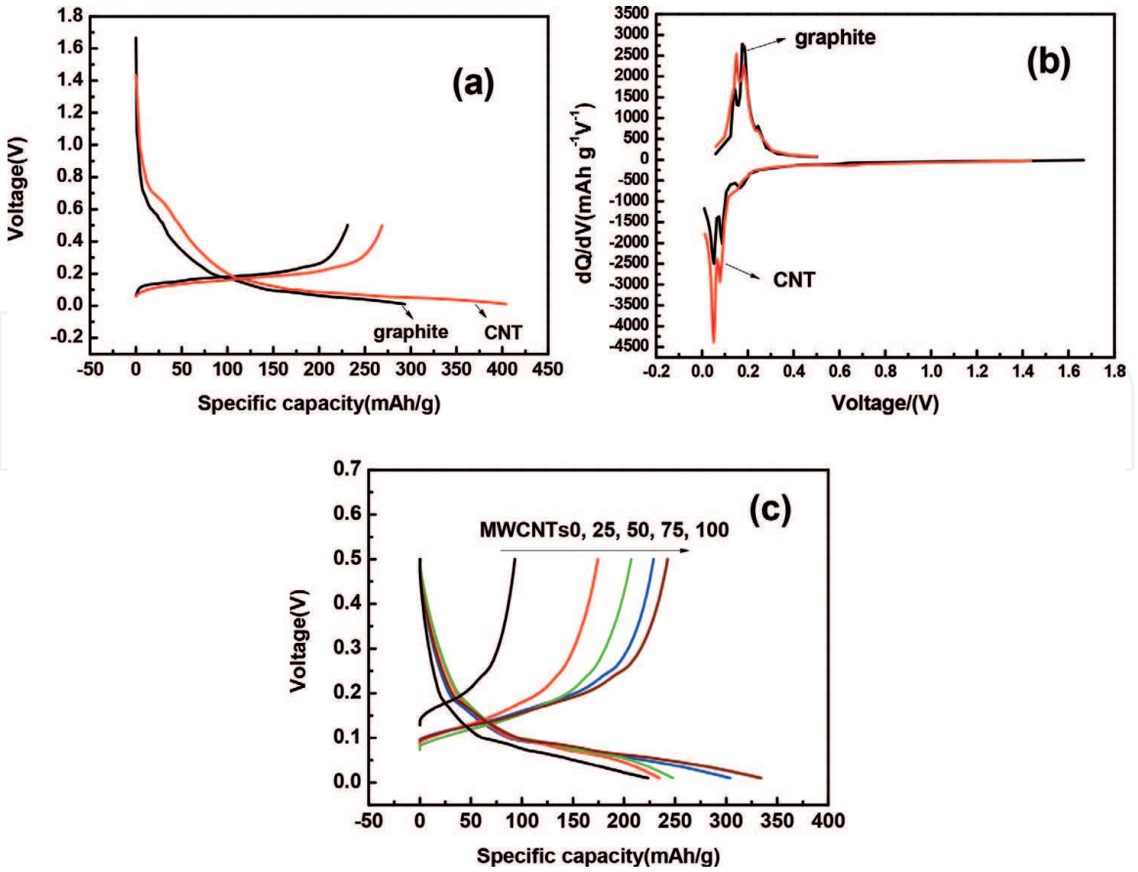

Figure 8.
The first charge-discharge curves of MWCNTs and graphite electrodes before being predoping (a), the differential capacity versus voltage (dQ/dV) curves of the MWCNTs/Li and graphite/Li coin cells (b) and the first charge curves of MWCNTs/graphite electrodes with different content of MWCNT at a prelithiation time of 60 min (c).

voltage plateau of SEI film formation is at about 0.7 V too. Meanwhile, MWCNTs have a higher irreversible capacity and first discharge capacity than graphite. **Figure 8(b)** shows the differential capacity versus voltage (dQ/dV) curves of MWCNTs and graphite half-cells. Three stages of lithium-ion intercalation voltage were local on 0.16, 0.08, and 0.055 V, respectively. **Figure 8(c)** shows the first delithiation (charge) capacity of CNT0, CNT25, CNT50, CNT75, and CNT100 at 60 min prelithiation time. In the same prelithiation time, the open-circuit voltage (OCV) of pure graphite half-cell was significantly superior to other half-cells. The delithiation capacity increases with the gradual increase of MWCNTs, which indicates the kinetics of intercalation of MWCNTs is higher than pure graphite.

Figure 9(a–e) showed the galvanostatic charge-discharge curves of LIC0, LIC25, LIC50, LIC75, and LIC100 at different current densities, respectively. The tests were performed using two-electrode system at voltage profile of 2–4 V. The energy density of LICs can be calculated by Esp = (Csp*V2)/2 (Csp represents the specific capacitance and V represents the discharge potential excluding IR drop). The power density of LICs can be calculated by Psp = Esp/t (t represents the discharge time), and the specific capacitance Csp can be calculated by the formula C = (2I*t)/(m*ΔV) (I represents the discharge current, m is the active material mass of a single pole, ΔV is the potential of discharge, and t is the discharge time). The charge-discharge curves of LIC25 showed a good linear relationship and exhibited a shape of isosceles triangle. The LIC25 had the longest discharge time than other LICs and showed good capacitance characteristics. Meanwhile, the charge-discharge curves of LIC75 also showed a good linear relationship and

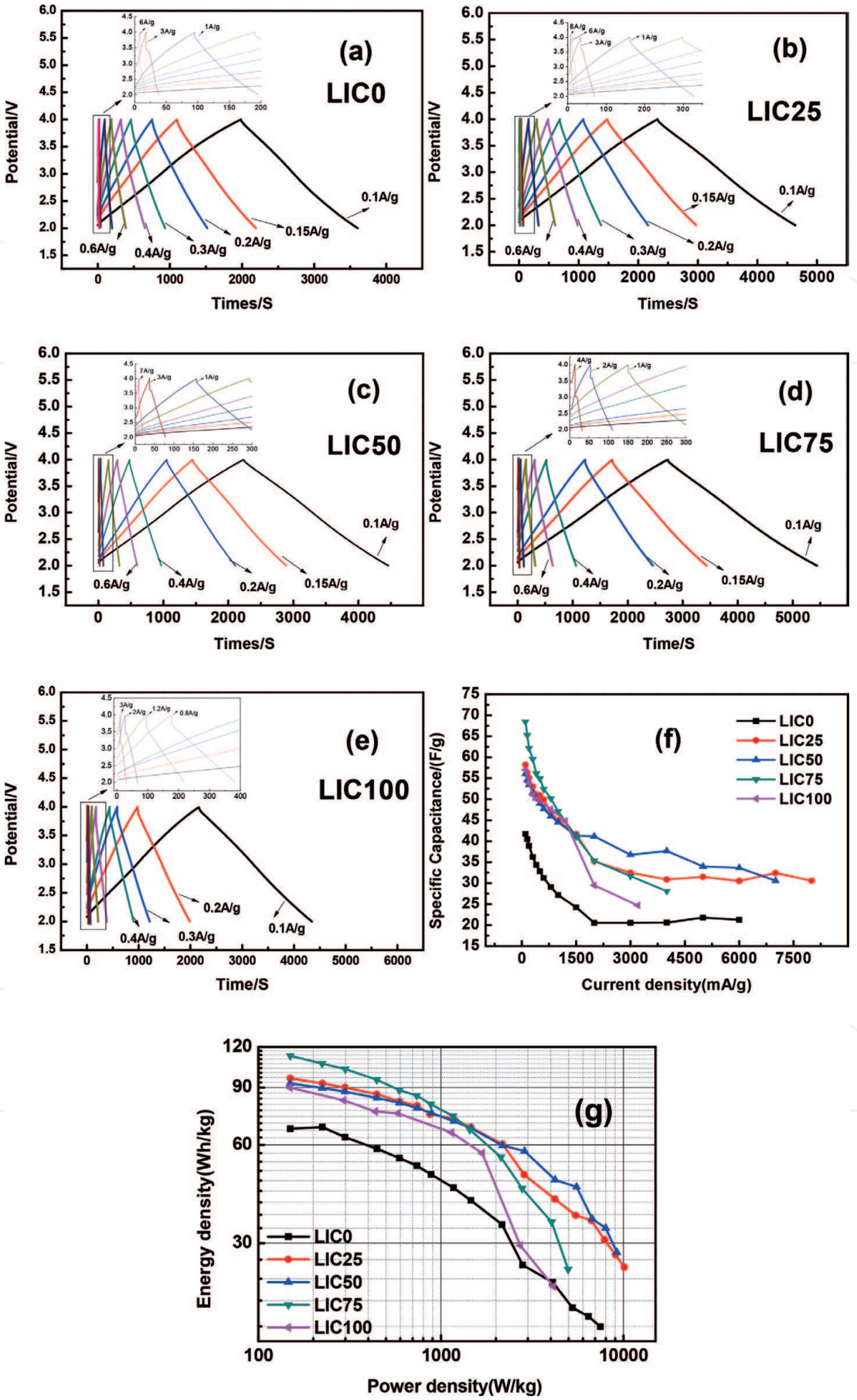

Figure 9.
Galvanostatic charge-discharge curves of lithium-ion capacitors with different content of WCNT at a different current density, (a) LIC0, (b) LIC25, (c) LIC50, (d) LIC75, (e) LIC100, and specific capacitance with different current density (f), the ragone plots for the LICs (g).

exhibited high power performance. On the contrary, the charge-discharge curves of LIC0 and LIC100 presented a distorted shape, and the internal resistance obviously increases with the improving current density and the discharge time is obviously shortened, which related a poor power density. Generally, the power density of LICs is determined by the negative materials; when the negative electrode consists of pure graphite, the rate of intercalation and deintercalation of lithium ions is slow, resulting in a poor power density. The intercalation and deintercalation rate of lithium ions will be accelerated with the addition of MWCNTs. However, excessive amounts of carbon nanotubes will consume large amounts of lithium ions, and the formation of thick solid electrolyte interface (SEI) film will greatly impede the migration of lithium ions. That is, the appropriate MWCNTs content to improve the power density is of crucial importance.

Figure 9(f) showed the specific capacitance of LICs at various current densities. The LIC25 showed higher discharging specific capacitance and rate performance than other LICs. **Figure 9(g)** showed the ragone plots of LICs. LIC25 presented the best electrochemical performance. The maximal energy density and power density of LIC25 reached 96 Wh/kg and 10.1 kW/kg in the range of current density from 0.1 to 8 A/g.

Figure 10 showed the charge and discharge cycle performance of LIC0 and LIC25. The 3000 cycles test was performed in the range of 2.2~3.8 V at the current density of 0.8 A/g. After 5000 cycles of constant current charge and discharge, the cycling performance of LIC0 drops significantly, which is related to the cracking and pulverization of graphite materials, lithium, and organic solvents common into the graphite layer, and then influences the performance of cycle. As opposed to LIC0, the capacitance retention of LIC25 still holds 86%, the charge and discharge curves without twist and distortion, which still maintained a good isosceles triangle shape and shows good cycle performance.

4.3 Conclusions

In the chapter, lithium-ion capacitors have been assembled with prelithiated MWCNTs/graphite composite as anode and activated carbon as cathode. The results showed that LICs with prelithiated exhibit excellent electrochemical performance. Especially, the LIC25 exhibited optimal electrochemical performance, with a specific capacitance of 58.2 F/g at current density of 0.1 A/g, and the maximal energy and power density reached 96 Wh/kg and 10.1 kW/kg in the range of current

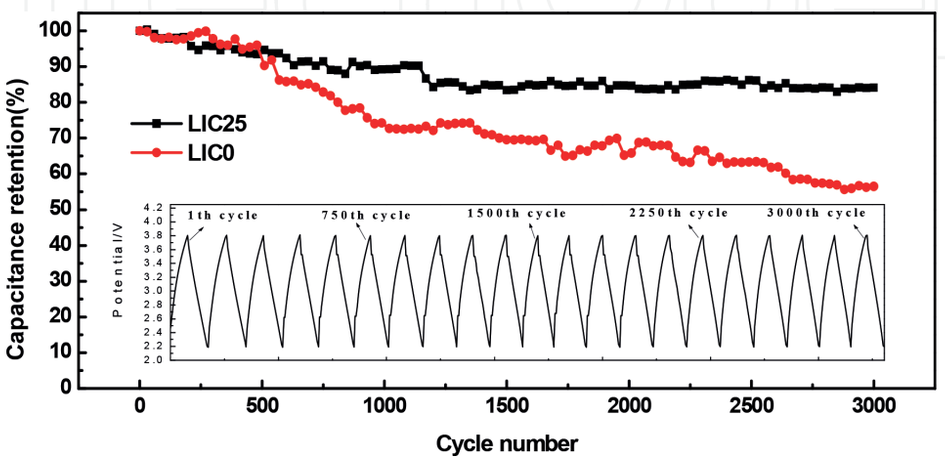

Figure 10.
Long-term cycle performance for the LIC in the voltage range of 2.2~3.8 V at 800 mA/g current density.

density from 0.1 to 8 A/g, respectively. After 3000 charge-discharge cycles, the LIC25 maintained about 86% capacity retention rate. Therefore, the LICs with the prelithiated MWCNTs/graphite composite materials have a potential application for energy storage device.

Author details

Xiaogang Sun*, Wei Chen, Xu Li, Jie Wang, Hao Hu, Guodong Liang, Yapan Huang and Chengcheng Wei
College of Mechantronics Engineering, Nanchang University, Nanchang, China

*Address all correspondence to: xiaogangsun@163.com

References

[1] Miller JR, Simon P. Electrochemical capacitors for energy management. Science Magazine. 2008;**321**(5889):651-652

[2] Kang YJ, Kim B, Chung H, et al. Fabrication and characterization of flexible and high capacitance supercapacitors based on MnO_2/CNT/papers. Synthetic Metals. 2010;**160**(23):2510-2514

[3] Liu M, Zhang L, Han P, et al. Controllable formation of niobium nitride/nitrogen-doped graphene nanocomposites as anode materials for lithium-ion capacitors. Particle & Particle Systems Characterization. 2016;**32**(11):1006-1011

[4] Wang H, Zhang Y, Ang H, et al. A high-energy lithium-ion capacitor by integration of a 3D interconnected titanium carbide nanoparticle chain anode with a pyridine-derived porous nitrogen-doped carbon cathode. Advanced Functional Materials. 2016;**26**(18):3082-3093

[5] Hosseinzadeh E, Genieser R, Worwood D, et al. A systematic approach for electrochemical-thermal modelling of a large format lithium-ion battery for electric vehicle application. Journal of Power Sources. 2018;**382**:77-94

[6] Hao ZQ, Cao JP, Wu Y, et al. Preparation of porous carbon sphere from waste sugar solution for electric double-layer capacitor. Journal of Power Sources. 2017;**361**:249-258

[7] Ren JJ, Su LW, Qin X, et al. Pre-lithiated graphene nanosheets as negative electrode materials for Li-ion capacitors with high power and energy density. Journal of Power Sources. 2014;**264**(264):108-113

[8] Fan K, Tian Y, Zhang X, et al. Application of stabilized lithium metal powder and hard carbon in anode of lithium–sulfur battery. Journal of Electroanalytical Chemistry. 2016;**760**:80-84

[9] Du H, Yang H, Huang C, et al. Graphdiyne applied for lithium-ion capacitors displaying high power and energy densities. Nano Energy. 2016;**22**:615-622

[10] Sun X, Zhang X, Liu W, et al. Electrochemical performances and capacity fading behaviors of activated carbon/hard carbon lithium ion capacitor. Electrochimica Acta. 2017;**235**:158-166

[11] Amatucci GG, Badway F, Pasquier AD, et al. An asymmetric hybrid nonaqueous energy storage cell. Journal of the Electrochemical Society. 2001;**148**(8):A930-A939

[12] Pasquier AD, Plitz I, Menocal S, et al. A comparative study of Li-ion battery, supercapacitor and nonaqueous asymmetric hybrid devices for automotive applications. Journal of Power Sources. 2003;**115**(1):171-178

[13] Dahn JR, Steel JA. Energy and capacity projections for practical dual-graphite cells. Journal of the Electrochemical Society. 2000;**147**(3):899-901

[14] Yoshino A, Tsubata T, Shimoyamada M, et al. Development of a lithium-type advanced energy storage device. Journal of the Electrochemical Society. 2004;**151**(12):A2180-A2182

[15] Sang-Wook W, Dokko K, Nakano H, et al. Bimodal porous carbon as a negative electrode material for lithium-ion capacitors. Electrochemistry. 2007;**75**(8):635-640

[16] Lee SW, Yabuuchi N, Gallant BM, et al. High-power lithium batteries

from functionalized carbon-nanotube electrodes. Nature Nanotechnology. 2010;**5**(7):531-537

[17] Jin Z, Liu X, Jing W, et al. Different types of pre-lithiated hard carbon as negative electrode material for lithium-ion capacitors. Electrochimica Acta. 2016;**187**:134-142

[18] Zhang P, Ma J, Mani S, et al. High Performance Anode Material for Lithium-Ion Battery: US, US7722991. 2010

[19] Byeon A, Glushenkov AM, Anasori B, et al. Lithium-ion capacitors with 2D Nb_2CT_x, (MXene)—Carbon nanotube electrodes. Journal of Power Sources. 2016;**326**:686-694

[20] Hsieh CL, Tsai DS, Chiang WW, et al. A composite electrode of tin dioxide and carbon nanotubes and its role as negative electrode in lithium ion hybrid capacitor. Electrochimica Acta. 2016;**209**:332-340

[21] Tropy NL, Cao W, Zheng JP. Comparison Study of Various Anode Materials for Li-Ion Capacitors[C]// Meeting Abstracts. The Electrochemical Society. 2014;(2):227-227

[22] Jayasinghe R, Thapa AK, Dharmasena RR, et al. Optimization of multi-walled carbon nanotube based CF_x, electrodes for improved primary and secondary battery performances. Journal of Power Sources. 2014;**253**(5):404-411

[23] Howe JY, Boatner LA, Kolopus JA, et al. Vacuum-tight sample transfer stage for a scanning electron microscopic study of stabilized lithium metal particles. Journal of Materials Science. 2012;**47**(3):1572-1577

[24] Kim M, Xu F, Jin HL, et al. A fast and efficient pre-doping approach to high energy density lithium-ion hybrid capacitors. Journal of Materials Chemistry A. 2014;**2**(26):10029-10033

[25] Park H, Kim M, Xu F, et al. In situ synchrotron wide-angle X-ray scattering study on rapid lithiation of graphite anode via direct contact method for Li-ion capacitors. Journal of Power Sources. 2015;**283**:68-73

[26] Aurbach D, Levi MD, Elena Levi A, et al. Failure and stabilization mechanisms of graphite electrodes. Journal of Physical Chemistry B. 1997;**101**(12):2195-2206

[27] Ng SH, Vix-Guterl C, Bernardo P, et al. Correlations between surface properties of graphite and the first cycle specific charge loss in lithium-ion batteries. Carbon. 2009;**47**(3):705-712

[28] Spahr ME, Buqa H, Würsig A, et al. Surface reactivity of graphite materials and their surface passivation during the first electrochemical lithium insertion. Journal of Power Sources. 2006;**153**(2):300-311

[29] Gao X, Zhan C, Yu X, et al. A high performance lithium-ion capacitor with both electrodes prepared from Sri Lanka graphite ore. Materials. 2017;**10**(4):414

[30] Barcellona S, Ciccarelli F, Iannuzzi D, et al. Overview of lithium-ion capacitor applications based on experimental performances. Electric Machines & Power Systems. 2016;**44**(11):1248-1260

[31] Khomenko V, Raymundo-Piñero E, Béguin F. High-energy density graphite/AC capacitor in organic electrolyte. Journal of Power Sources. 2008;**177**(2):643-651

[32] Sivakkumar SR, Nerkar JY, Pandolfo AG. Rate capability of graphite materials as negative electrodes in lithium-ion

capacitors. Electrochimica Acta. 2010;**55**(9):3330-3335

[33] Sun XG, Qiu ZW, Chen L, et al. Industrial synthesis of whisker carbon nanotubes. Materials Science Forum. 2016;**852**:514-519

[34] Zhang J, Shi Z, Wang J, et al. Composite of mesocarbon microbeads/hard carbon as anode material for lithium ion capacitor with high electrochemical performance. Journal of Electroanalytical Chemistry. 2015;**747**:20-28

[35] Zhang J, Shi Z, Wang C. Effect of pre-lithiation degrees of mesocarbon microbeads anode on the electrochemical performance of lithium-ion capacitors. Electrochimica Acta. 2014;**125**(12):22-28

[36] Ai G, Wang Z, Zhao H, et al. Scalable process for application of stabilized lithium metal powder in Li-ion batteries. Journal of Power Sources. 2016;**309**:33-41